

Frequency and amplitude stabilized terahertz quantum cascade laser as local oscillator

Y. Ren,^{1,2,3,a)} D. J. Hayton,⁴ J. N. Hovenier,¹ M. Cui,⁴ J. R. Gao,^{1,4,a)} T. M. Klapwijk,¹ S. C. Shi,² T.-Y. Kao,⁵ Q. Hu,⁵ and J. L. Reno⁶

¹Kavli Institute of NanoScience, Delft University of Technology, Lorentzweg 1, 2628 CJ Delft, The Netherlands

²Purple Mountain Observatory (PMO), Chinese Academy of Sciences, 2 West Beijing Road, Nanjing, JiangSu 210008, China

³Graduate School, Chinese Academy of Sciences, 19A Yu Quan Road, Beijing 100049, China

⁴SRON Netherlands Institute for Space Research, Sorbonnelaan 2, 3584 CA Utrecht, The Netherlands

⁵Department of Electrical Engineering and Computer Science, Massachusetts Institute of Technology (MIT), Cambridge, Massachusetts 02139, USA

⁶Sandia National Laboratories, Albuquerque, New Mexico 87185-0601, USA

(Received 19 July 2012; accepted 22 August 2012; published online 6 September 2012)

We demonstrate an experimental scheme to simultaneously stabilize the frequency and amplitude of a 3.5 THz third-order distributed feedback quantum cascade laser as a local oscillator. The frequency stabilization has been realized using a methanol absorption line, a power detector, and a proportional-integral-derivative (PID) loop. The amplitude stabilization of the incident power has been achieved using a swing-arm voice coil actuator as a fast optical attenuator, using the direct detection output of a superconducting mixer in combination with a 2nd PID loop. Improved Allan variance times of the entire receiver, as well as the heterodyne molecular spectra, are demonstrated. © 2012 American Institute of Physics. [<http://dx.doi.org/10.1063/1.4751247>]

A terahertz (THz) quantum cascade laser (QCL) is the most promising solid-state source as the local oscillator (LO) for a high resolution heterodyne receiver operating at frequencies above 2 THz and, in particular, for a multi-pixel array receiver because of its high output power (typically mW).^{1,2} Among different types of applications, a super-THz heterodyne receiver plays a vital role in astronomical observations, for instance to map a large number of fine structures and molecular lines associated with the formation of stars and planets in the Milky Way and nearby galaxies.³ Those spectral lines at high frequencies are typically narrow (\leq a few MHz). Furthermore, the signals are, in general, very weak and deeply embedded within the noise.³

The narrow spectral lines require either frequency or phase stabilization of a local oscillator. Since the intrinsic linewidth of a THz QCL is much narrower ($<$ kHz)⁴ than typical astronomical lines, frequency locking of a QCL will be sufficient. Until now, a considerable amount of progress has been made to achieve either phase locking or frequency locking to a THz QCL.⁵⁻⁷ In essence, these experiments have established that the THz QCL, like other solid-state oscillators, is a voltage-controlled oscillator (VCO) whose frequency is determined by a control DC voltage.

The weak signal lines require a long integration time during an observation and of course a high sensitivity of the mixer. The effective integration time is limited by the stability of the entire receiver, which is characterized by the Allan variance time for a given measurement bandwidth.⁸ For a receiver based on a superconducting hot electron bolometer (HEB) mixer, the stability is dominated by the amplitude stability of the incident LO power.⁹ It is known that the output power of a THz QCL is determined by both DC bias and

operating temperature. Thus, any fluctuation or drift either in the bias or in the temperature may give rise to output power fluctuation. The power stability becomes problematic when the QCL is operated in a pulse tube cryocooler, where temperature variations and fluctuations are intrinsically present. Furthermore, the DC bias regulates the emission frequency of the laser at a given temperature. In order to stabilize the frequency and amplitude of the laser simultaneously, another means of tuning, besides from the DC bias, is desired, especially when the frequency and amplitude fluctuations are anti-correlated to the bias.

In this letter, we apply a swing-arm actuator placed in the optical beam path to block part of the QCL beam in order to stabilize the incident power, using in this case a 3.5 THz QCL. The amplitude stabilization loop consists of a proportional-integral-derivative (PID) controller and it takes advantage of the direct power detection of a HEB mixer. As demonstrated in Ref. 9, by stabilizing the power from a THz gas laser used as a LO, this technique can improve the stability of a 2.5 THz heterodyne receiver drastically. The frequency of the QCL is locked to a methanol (CH₃OH) absorption line. By implementing these two stabilization schemes simultaneously, we achieve a fully stabilized heterodyne receiver, which is further characterized by Allan variance and heterodyne spectroscopy.

The LO used is a third-order distributed feedback (DFB) QCL based on a metal-metal, lateral corrugated waveguide, which, until now, is the most advanced THz QCL for the purpose of local oscillators.¹⁰ Its unique features are tunable single mode frequency operation and low-divergent main lobe in the beam. The latter, as a result of the grating structure that behaves as a linear phased array antenna, is crucial for better coupling of the radiation power between the laser and an HEB mixer. Such 3rd DFB lasers have the potential of higher operating temperatures ($>$ 77 K) and lower DC

^{a)}Authors to whom correspondence should be addressed. Electronic addresses: y.ren@tudelft.nl and j.r.gao@tudelft.nl.

dissipation power (<1 W) because of the metal-metal waveguide structure. In detail, the laser used consists of a $10\ \mu\text{m}$ thick MBE grown GaAs/AlGaAs active region with 27 periods of gratings and a total length of $1070\ \mu\text{m}$. It radiates a single mode emission line tunable from 3452.0 to $3450.8\ \text{GHz}$ by varying the bias voltage from $13.9\ \text{V}$ to $14.9\ \text{V}$. Its maximum output power is $0.8\ \text{mW}$ at an operating temperature of $\sim 12\ \text{K}$. The divergence of the main beam is about 12° in both vertical and horizontal directions. The same laser has been used for demonstrating heterodyne molecular spectroscopy with tuning capability¹¹ and frequency locking.¹²

As the mixer, we employ a superconducting NbN HEB mixer with a nanobridge of $0.2 \times 2\ \mu\text{m}^2$ in size, operated at liquid He temperature ($4.2\ \text{K}$) and requiring an optimal LO power of $150\ \text{nW}$ at the detector itself.¹³ The HEB mixer is the most sensitive heterodyne detector operated at frequencies between $1.5\ \text{THz}$ and $6\ \text{THz}$. The mixer performance such as the mixing conversion gain and intermediate frequency (IF) output power depends strongly on the LO power. Thus, any variation in LO power can affect the operating state and thus induce instability in the mixing performance.

Fig. 1 shows the complete setup for the amplitude and frequency stabilization experiment as well as for the heterodyne spectroscopy measurements. We start with the setup required only for the stabilization experiment. The QCL is operated in a pulse tube cryocooler at a stabilized operating temperature of $16\ \text{K}$. The THz radiation from the QCL is first focused with a high-density polyethylene (HDPE) lens, and then passes through the voice coil attenuator. Subsequently, the QCL signal is split into two beams by a $13\ \mu\text{m}$ thick Mylar beam splitter, where the reflected signal works as a LO to pump the HEB mixer, while the transmitted beam is used for the frequency locking. The frequency locking loop consists of a gas cell (Gas cell 1) at room temperature, in

which a methanol absorption line is used as the frequency reference. Furthermore, a 2nd superconducting NbN hot electron bolometer is operated only as a direct power detector, together with a PID controller and a lock-in amplifier. The technique used for the frequency locking is very similar to that reported in Refs. 12 and 14. The voice coil actuator together with a second PID feedback loop is used to realize the amplitude stabilization, where the DC current of the voltage biased HEB mixer is used as a power reference signal. If the incident LO power fluctuates, a feedback current will be generated to drive the voice coil that acts as a variable optical attenuator by interrupting partial LO beam to maintain a constant DC current of the mixer. The voice coil is superior to a rotational polarizer since it responds fast (up to $1\ \text{kHz}$), and has the advantage of high resolution and full dynamic range. This technique can reduce not only the instability of the LO amplitude but also other instability factors like atmospheric turbulence in the LO path and LO mechanical instability. To characterize the stability of the receiver and measure Allan variance times, a hot/cold ($295/77\ \text{K}$) black-body load is applied as the input signal. The IF signal from the HEB mixer is amplified by a wide-band cryogenic amplifier, followed by two room temperature amplifiers, with a $100\ \text{MHz}$ bandwidth ($1.4\text{--}1.5\ \text{GHz}$) bandpass filter. The IF signal is further sampled by a power meter.

For the frequency locking experiment, a bias circuit for the QCL combines three input signals, where a DC bias voltage, an AC sinusoidal modulation signal ($\sim 1\ \text{kHz}$), and a feedback control signal are employed to independently control the laser.^{12,14} By feeding the output current of the HEB power detector to a lock-in amplifier, the derivative signal of the absorption profile is obtained. Then, a feedback signal from a PID controller is used to actively lock this derivative signal, maintained at zero value. In this way, the laser frequency is stabilized to a particular methanol absorption line. And this frequency locking alone has been realized previously for a QCL in Refs. 12 and 14.

To characterize the stabilization, we monitor the frequency fluctuation of the QCL by the output of the lock-in amplifier, the amplitude fluctuation of the incident power by the DC current of the HEB mixer, and the stability of the HEB receiver by the output of the IF amplifier chain in four different operation modes, covering (1) free running; (2) only frequency stabilized; (3) only amplitude stabilized; and (4) both frequency and amplitude stabilized. Fig. 2 shows the key results by plotting the three signals within four operation modes. In the free running mode, the observed low frequency fluctuations and drift in the lock-in signal are a result of the frequency noise of the laser due to external contributions mainly from the temperature variations of the cryocooler. The contribution of the cryocooler also induces amplitude instability,¹⁵ reflected by the fluctuations of the HEB mixer current and of the IF output power. In the second operating mode when the frequency stabilization loop is enabled, the lock-in signal becomes well stabilized and is maintained at the set point of zero, which implies that the QCL frequency is fully stabilized. However, in this case, the fluctuations in the amplitude of the QCL increase, reflected by those in the HEB current. Also the fluctuations in the mixer IF output are increased as a result of the fluctuations

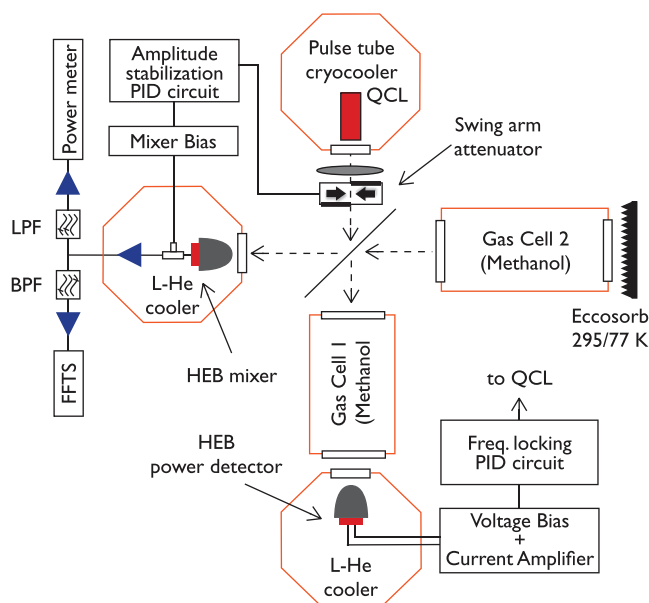


FIG. 1. Schematic of the measurement setup for demonstrating both amplitude and frequency stabilization of a $3.5\ \text{THz}$ QCL as local oscillator for a heterodyne receiver. It is also the setup for the Allan variance and spectroscopic measurements.

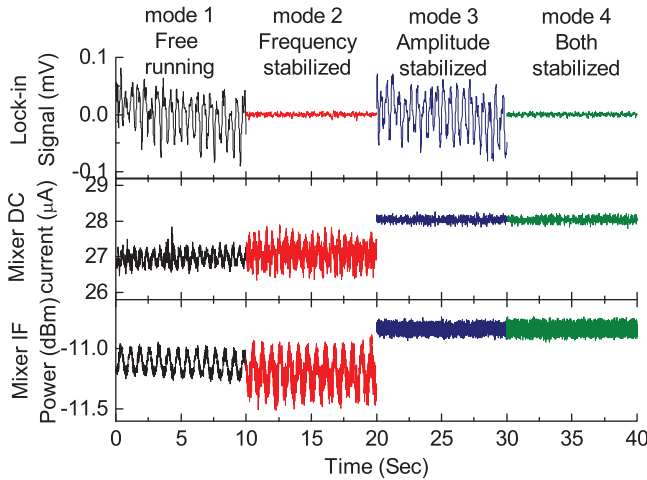


FIG. 2. The lock-in amplifier signal, reflecting stability of the QCL frequency, the DC current of the HEB mixer, reflecting the QCL amplitude, and the output power of the IF amplifier chain, reflecting the stability of the entire receiver, versus time for four different operating modes of (1) the free running; (2) only frequency stabilized; (3) only amplitude stabilized; and (4) both frequency and amplitude stabilized.

of the LO power. In the third mode when the amplitude stabilization loop becomes active, but the frequency stabilization loop is disabled, as expected, the fluctuations in the lock-in signal remain the same as in the free-running case, while the HEB mixer current is well stabilized and locked to a constant value. Consequently, the mixer IF power becomes stabilized with no drift and with much less fluctuations. In the last operating mode when both the amplitude and frequency stabilization loops are enabled, as shown in Fig. 2, not only the lock-in signal but also the HEB mixer current as well as mixer IF power are stabilized. We therefore conclude that we succeed in achieving the simultaneous frequency and amplitude stabilization of the QCL.

In the 2nd operation mode, when only the frequency is locked, the amplitude fluctuates more. This suggests that the fluctuation or the frequency noise is anti-correlated to the fluctuation in the amplitude through the QCL bias voltage. The underlying physics is relatively straightforward. It is known that both frequency and output power of a THz QCL are a function of both DC bias and operating temperature. The emission power, in general, decreases if either the temperature increases or the DC bias decreases, which is true in the operating regime of our QCL. However, the frequency behavior can be different and is device dependent. Based on our previous measurement on the same QCL,¹¹ we find that the frequency decreases if the temperature increases or the voltage increases. Thus, a small increase in temperature as a distortion will decrease the emission frequency as well as the amplitude. In response, the frequency locking loop through the PID will generate a negative voltage signal to compensate for the frequency decrease. However, as a result, the amplitude will further decrease. In other words, the fluctuations in the amplitude will increase as shown in Fig. 2. In contrast, for the 3rd operating mode, when the voice coil is applied to stabilize the amplitude, no effect has been seen to the frequency fluctuations since the amplitude adjustment is completely independent of the QCL operation.

The linewidth of the QCL is estimated by transforming the variation in voltage of the lock-in signal in the time domain into the frequency domain.¹² As a result, we obtain a free running linewidth of about 1.5 MHz, while the locked linewidth is around 35 kHz in the fully stabilized state. The linewidth reduction factor is the same as one reported in Ref. 12, and the linewidth value has the same order of magnitude as well (18 kHz measured previously), which is sufficiently narrow for practical use as a local oscillator. The difference in the absolute value can be due to the different operating conditions of the QCL.

We also perform an Allan variance measurement in the total power (continuum) mode to quantify the effect of the stability of the amplitude to the entire receiver. Allan variance is a well-known, powerful tool for characterizing the stability of a system.¹⁶ We measure the Allan variance $\sigma_A^2(\tau)$ of the normalized IF output power, given by $\sigma_A^2(\tau) \equiv 1/2 \sigma(\tau)^2$, where σ^2 is the average squared standard deviation of each number from its mean and τ is the sampling period. The measured $\sigma_A^2(\tau)$ for the entire receiver is plotted as a function of the sampling time in Fig. 3 for three different measurement conditions. For comparison, the radiometer equation for an effective noise fluctuation bandwidth of 13.5 MHz is also plotted. The Allan time when the QCL in free running state is below 0.01 s. And the measurement shows an extremely unstable behavior, suggested by the presence of strong oscillations attributed to the low frequency temperature oscillations in the pulse tube cryocooler. In contrast, the Allan time from a both frequency and amplitude stabilized receiver is about 0.3 s for a measured 13.5 MHz bandwidth. An improvement with a factor of more than 30 is achieved by introducing the amplitude stability in addition to the frequency locking. Furthermore, the data from the HEB in the superconducting state show the stability of the entire IF amplifier chain, which gives a total power Allan time at around 2 s. The Allan times for the stabilized receiver and from the superconducting state are all shorter than reported in Ref. 9 indicating a non-optimized IF amplifier chain as the main limiting factor. The improvement can

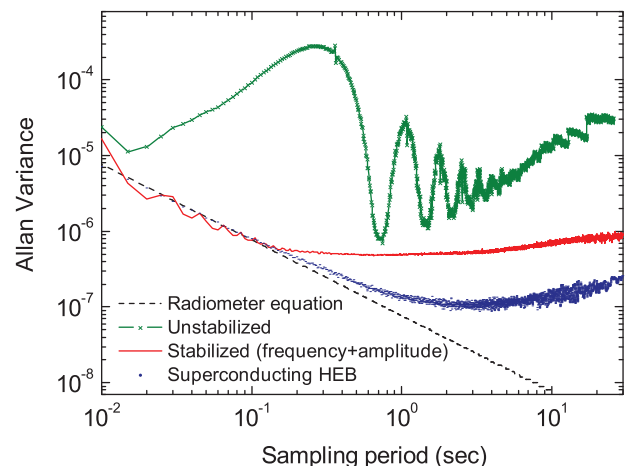


FIG. 3. Measured total power Allan variance of the entire receiver as a function of sampling period when the QCL LO is free running, fully stabilized, and when the HEB in a superconducting state with no electrical bias and no LO power. The radiometer equation for an effective noise fluctuation bandwidth of 13.5 MHz is also shown.

be realized by carefully designing and arranging the set-up with respect to, for example, the air turbulence and the temperature stabilization of the room temperature IF amplifiers.

To further verify the performance of the stabilized receiver, we perform heterodyne molecular spectroscopic measurements. The measurement setup is also sketched in Fig. 1, where the HEB mixer and QCL parts are the same as the one described for the stability experiment, except for the input signal and IF readout (the backend). In this case, the signal source is a combination of a methanol gas cell (Gas cell 2) and a hot/cold blackbody load. The same IF amplifier chain is used, but with a 0–1.5 GHz low pass filter in between. The spectrum is recorded by a fast Fourier transform spectrometer (FFTS). In fact, two types of spectroscopic measurements are performed. One is to measure the methanol emission lines using the QCL-HEB receiver with both frequency and amplitude stabilized. The main figure in Fig. 4 plots methanol emission lines in the intermediate frequencies between 0 and 1.5 GHz, which are down converted from 3.5 THz methanol lines. Also, a modeled spectrum for the same frequency range is plotted in the main figure. It can be seen that an excellent agreement between the calculation and the data is obtained with respect to both the line frequencies and the relative intensities. Because of the amplitude stabilization, one measurement with only three traces¹¹ can lead to a reliable spectrum. Averaging of many different measurements is not required. The second type is to measure, with amplitude stabilization for the QCL, methanol emission lines over an extended time interval with and without frequency locking. The inset of Fig. 4 shows two sets of measured methanol lines in the frequency range of 0.8–1.1 GHz for a gas pressure reduced to 0.12 mbars, using a 3 s integration time for each data trace. Each spectrum is re-measured after a 1 h interval. We find that two spectra can overlap well when both frequency and amplitude stabilized, while there is a frequency offset of about 5 MHz between the two spectra when only amplitude is stabilized (but no frequency stabilization). The latter implies a frequency

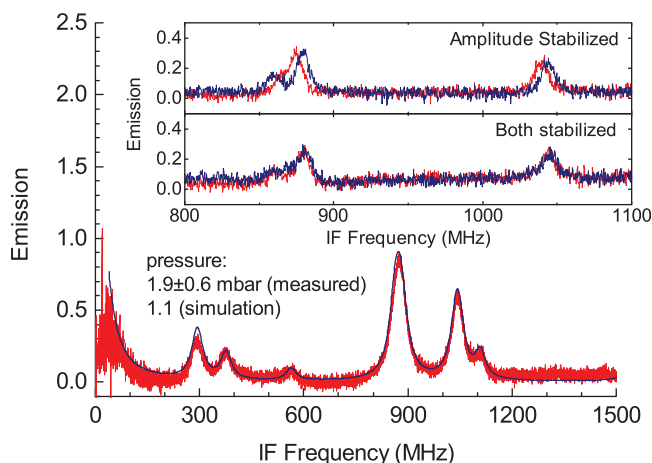


FIG. 4. In the main figure: a measured 3.5 THz methanol spectrum in the intermediate frequencies when both frequency and amplitude of the LO is stabilized (in red). The gas pressure is 1.9 ± 0.6 mbars. A simulated methanol spectrum with a pressure of 1.1 mbars is in blue. One inset shows a methanol spectrum when the LO is only amplitude stabilized (the upper one), measured twice with 1 h interval time. The 2nd inset shows a methanol spectrum when both amplitude and frequency are stabilized. The gas pressure is reduced to 0.12 ± 0.05 mbars.

drift of the LO. It proves that the LO frequency can indeed be locked, which is crucial for the spectroscopic measurement. It is worthwhile to note that, because of the full stabilization, we can resolve fine spectral lines as narrow as 10 MHz at the low gas pressure.

In conclusion, we succeeded in demonstrating a fully stabilized 3.5 THz QCL, both in its amplitude and frequency, as a local oscillator operated in a pulse tube cryocooler for a heterodyne receiver. The frequency is locked to a methanol absorption line through the PID and the bias voltage, resulting in a linewidth as narrow as 35 kHz. The amplitude is stabilized by applying a swing-arm actuator blocking part of the LO beam for rapid feedback LO intensity control. The effectiveness of the amplitude stabilization and frequency locking is supported by the improved Allan time of the entire heterodyne receiver and also the high-resolution heterodyne spectroscopic measurements.

The work is partly supported by CAS-KNAW Joint PhD Training Programme, and by the AMSTAR+ project of RadioNet under FP7, NWO, and NATO SFP. The work at PMO is supported in part by the National Natural Science Foundation of China under Grant 11127903 and 10933005, by CAS program under Grant KJXC2-EW-T05, and by the CAS Key Laboratory of Radio Astronomy. The work at MIT is supported by NASA and NSF. The work at Sandia was performed, in part, at the Center for Integrated Nanotechnologies. Sandia National Laboratories is a multi-program laboratory managed and operated by Sandia Corporation.

¹R. Köhler, A. Tredicucci, F. Beltram, H. E. Beere, E. H. Linfield, A. G. Davies, D. A. Ritchie, R. C. Iotti, and F. Rossi, *Nature* **417**, 156 (2002).

²B. S. Williams, *Nat. Photonics* **1**, 517 (2007).

³E. F. van Dishoeck and A. G. G. M. Tielens, "Space-borne observations of the lifecycle of interstellar gas and dust," in *The Century of Space Science*, edited by J. A. Bleeker, J. Geiss, and M. C. E. Hube (Kluwer Academic Publishers, 2001), p. 607.

⁴M. S. Vitiello, L. Consolino, S. Bartalini, A. Taschin, A. Tredicucci, M. Inguscio, and P. De Natale, *Nat. Photonics* **6**, 525 (2012).

⁵D. Rabanus, U. U. Graf, M. Philipp, O. Ricken, J. Stutzki, B. Vowinkel, M. C. Wiedner, C. Walther, M. Fischer, and J. Faist, *Opt. Express* **17**, 1159 (2009).

⁶A. A. Danylov, T. M. Goyette, J. Waldman, M. J. Coulombe, A. J. Gatesman, R. H. Giles, W. D. Goodhue, X. Qian, and W. E. Nixon, *Opt. Express* **17**, 7525 (2009).

⁷S. Barbieri, P. Gellie, G. Santarelli, L. Ding, W. Maineult, C. Sirtori, R. Colombelli, H. Beere, and D. Ritchie, *Nat. Photonics* **4**, 636 (2010).

⁸D. W. Allan, *Proc. IEEE* **54**, 221 (1966).

⁹D. J. Hayton, J. R. Gao, J. W. Kooi, Y. Ren, W. Zhang, and G. de Lange, *Appl. Phys. Lett.* **100**, 081102 (2012).

¹⁰M. I. Amanti, G. Scalari, F. Castellano, M. Beck, and J. Faist, *Opt. Express* **18**, 6390 (2010).

¹¹Y. Ren, J. N. Hovenier, R. Higgins, J. R. Gao, T. M. Klapwijk, S. C. Shi, B. Klein, T.-Y. Kao, Q. Hu, and J. L. Reno, *Appl. Phys. Lett.* **98**, 231109 (2011).

¹²Y. Ren, J. N. Hovenier, M. Cui, D. J. Hayton, J. R. Gao, T. M. Klapwijk, S. C. Shi, T.-Y. Kao, Q. Hu, and J. L. Reno, *Appl. Phys. Lett.* **100**, 041111 (2012).

¹³W. Zhang, P. Khosropanah, J. R. Gao, E. L. Kollberg, K. S. Yngvesson, T. Bansal, R. Barends, and T. M. Klapwijk, *Appl. Phys. Lett.* **96**, 111113 (2010).

¹⁴H. Richter, S. G. Pavlov, A. D. Semenov, L. Mahler, A. Tredicucci, H. E. Beere, D. A. Ritchie, and H.-W. Hübers, *Appl. Phys. Lett.* **96**, 071112 (2010).

¹⁵H. Richter, A. D. Semenov, S. G. Pavlov, L. Mahler, A. Tredicucci, H. E. Beere, D. A. Ritchie, K. S. Il'in, M. Siegel, and H.-W. Hübers, *Appl. Phys. Lett.* **93**, 141108 (2008).

¹⁶J. W. Kooi, G. Chattopadhyay, M. Thielman, T. G. Phillips, and R. Schieder, *Int. J. Infrared Millim Waves* **21**, 689 (2000).